

Thermo-Sensitizing Potential Of 5-FU-Entrapped Edge-Activating Transfersomes: Optimization, Characterization, And Biological Evaluation

Nidhi Jain^{1*}, Anup Kumar Chakraborty²

^{1*}Research Scholars, Department of Pharmacy, Oriental University, Indore, India.

²Professor, Department of Pharmacy, Oriental University, Indore, India.

***Corresponding Author:** Nidhi Jain,

*Research Scholars, Oriental University, Indore, India. nidhijain.btpc@gmail.com

Citation: Nidhi Jain, et.al (2022). Thermo-Sensitizing Potential Of 5-FU-Entrapped Edge-Activating Transfersomes: Optimization, Characterization, And Biological Evaluation, *Educational Administration: Theory and Practice*, 28(4) 590-597
Doi: 10.53555/kuey.v28i4.10624

ARTICLE INFO

ABSTRACT

The topical delivery potential of newly developed nanocarrier-based drug delivery systems has been extensively explored for enhancing the retention time of anticancer agents at the site of application. These systems are particularly advantageous for localized drug delivery, offering improved therapeutic efficacy with minimal systemic exposure. In this context, 5-fluorouracil (5-FU) was successfully encapsulated within a transfersosomal formulation utilizing 30% soya lecithin. The optimized ratio of 5-FU to soya lecithin was determined to be 1:1. The resulting 5-FU-loaded transfersomes exhibited favorable physicochemical properties, with an average particle size of 35.58 ± 0.56 nm, a polydispersity index (PDI) of 0.285 ± 0.125 , and a zeta potential of $+14.50 \pm 0.8$ mV. The formulation P-16 demonstrated the highest encapsulation efficiency, reaching $85.05 \pm 0.58\%$. Further characterization was carried out using Transmission Electron Microscopy (TEM), Fourier Transform Infrared Spectroscopy (FTIR), and X-ray Diffraction (XRD) analyses.

Keywords: Anticancer, 5-Fluorouracil, Transfersomes, Quality by Design (QbD), Box–Behnken Design, Soya Lecithin (30%)

INTRODUCTION

Topical drug delivery systems, including transdermal applications, offer several advantages over conventional drug delivery methods, particularly by bypassing first-pass metabolism. The topical application of 5-fluorouracil (5-FU) has garnered significant attention due to its anti-inflammatory, antioxidant, and immunomodulatory properties, which collectively contribute to its therapeutic potential in the treatment of UV-induced skin cancer. 5-FU effectively inhibits both photocarcinogenic cells and tumor-initiating cells in the skin. Its primary mechanism of action involves the inhibition of thymidylate synthase (TS), an essential enzyme in DNA synthesis, leading to disrupted DNA replication and cell cycle arrest. As a well-established and safe chemotherapeutic agent, 5-FU demonstrates high efficacy in managing skin malignancies through localized delivery.

Topical delivery of medications to the skin provides a targeted and efficient therapeutic approach for local dermatological conditions. Among the available formulations, hydrogels are particularly favored due to their non-greasy texture, hydrophilic nature, ease of application, and ability to be readily removed from the skin surface.

Transfersomal vesicles, known for their ultra-deformability, offer enhanced skin penetration compared to conventional liposomes. These vesicles facilitate drug permeation through the stratum corneum by adapting their shape under mechanical stress and navigating intercellular lipid pathways. The enhanced elasticity of transfersomes is attributed to the inclusion of suitable edge activators (surfactants), which modulate membrane fluidity and deformability. The rational selection and proportion of lipid components and surfactants are crucial for optimizing vesicle performance.

Cancer is a complex genetic disorder characterized by the uncontrolled proliferation and spread of abnormal cells in one or more tissues or organs. It typically arises following a series of genetic mutations that disrupt normal cellular regulatory mechanisms, allowing malignant cells to survive, multiply, and form tumors.

Prolonged exposure to UV radiation leads to photoaging, characterized by skin discoloration, wrinkles, loss of elasticity, and premature aging. It also contributes to the development of skin cancers such as melanoma, squamous cell carcinoma (SCC), and basal cell carcinoma (BCC). UV radiation induces inflammation, oxidative stress, DNA damage (e.g., cyclobutane pyrimidine dimers), and mutations in tumor suppressor genes like p53. Additionally, it promotes gene expression via intracellular signaling pathways, facilitating tumor progression. UV exposure also generates reactive oxygen species (ROS), which activate transcription factors such as AP-1 and NF- κ B, influencing cell proliferation and apoptosis.

MATERIAL AND METHODS

Materials

The drug 5-fluorouracil (5-FU) was procured from S.K. Traders, Indore. Tween 80, Rhodamine, and phospholipids (HPLC grade) were obtained from New Modern Chemical Corporation, Mumbai. Soya lecithin (30%) was purchased from HiMedia Laboratories, while Carbopol 940 and Span 80 were sourced from LOBA Chemie Pvt. Ltd., Mumbai, India. The marketed formulation of 5-FU (Flonida 1% cream) was procured from Rohan Chemist, Indore. All other chemicals and reagents used in the study were of analytical grade. Purified water from a Synergy UV water purification system (India) was used throughout the experimental procedures.

Preparation of Transfersome

Transfersomes were prepared following the method described by Patel et al. (2009), with slight modifications. The formulation utilized the thin-film hydration method combined with sonication. Briefly, the active anticancer drug 5-fluorouracil (5-FU), soya lecithin (30% phospholipid), and a non-ionic surfactant (Tween 80 or Span 80, serving as the edge activator) were dissolved in ethanol within a round-bottom flask (RBF). The mixture was then heated to approximately 55°C, and the organic solvent was gradually evaporated using a rotary evaporator to form a thin lipid film on the inner wall of the flask.

The thin film was allowed to dry completely over 12 hours to ensure complete solvent removal. Subsequently, the lipid film was hydrated with phosphate buffer (pH 7.4) and subjected to probe sonication at room temperature for approximately 30 minutes to reduce the vesicle size and achieve uniform transfersomal vesicles. The resulting suspension was further hydrated in phosphate buffer and stored at 2–8°C for 1 hour. The prepared transfersomes were stored in airtight containers for further characterization. Blank transfersomes (without 5-FU) were also prepared using the same method for comparative analysis.

Optimization of Drug Loaded Transfersomes

A Box–Behnken Design (BBD) combined with Response Surface Methodology (RSM) was employed using statistical software to investigate the influence of three critical formulation variables on the characteristics of 5-FU-loaded transfersomes. The selected independent variables included: (X₁) the ratio of soya lecithin (30%) to edge activator (Tween 80/Span 80), (X₂) sonication time, and (X₃) drug concentration (5-FU). The dependent responses evaluated were vesicle size (Y₁), entrapment efficiency (EE%) (Y₂), and drug loading (DL%) (Y₃).

The ranges for each variable were selected based on preliminary studies and literature reports [Nasr et al., 2015], ensuring the feasibility of the formulation process and the quality of the resulting transfersomes. The experimental design involved three factors and three levels, analyzed using 17 experimental runs. The resulting particle size ranged from 35.09 nm to 56.25 nm, entrapment efficiency ranged from 84.70% to 87.24%, and drug loading varied from 0.013% to 8.042%.

The quadratic polynomial equations generated to model the response surfaces were as follows:

Y₁ (Particle Size, PS):

$$Y_1 = 50.48 + 0.070X_1 - 3.81X_2 - 2.24X_3 - 0.98X_1X_2 + 0.070X_1X_3 - 2.89X_2X_3 - 4.20X_1^2 - 5.15X_2^2 - 3.15X_3^2 \dots (1)$$

Y₂ (Entrapment Efficiency, EE%):

$$Y_2 = 98.85 + 2.06X_1 - 0.46X_2 - 1.29X_3 + 0.085X_1X_2 - 0.071X_1X_3 + 0.013X_2X_3 - 1.02X_1^2 + 0.004X_2^2 + 0.014X_3^2 \dots (2)$$

Y₃ (Drug Loading, DL%):

$$Y_3 = 15.94 - 1.39X_1 + 0.050X_2 - 0.58X_3 + 0.042X_1X_2 + 0.051X_1X_3 + 0.018X_2X_3 - 0.81X_1^2 - 0.018X_2^2 + 0.003X_3^2 \dots (3)$$

FTIR Spectroscopy Analysis:

Infrared (IR) absorption spectroscopy was performed to analyze the functional groups of the drugs. Finely powdered samples of the drugs were triturated with dry potassium bromide (KBr) in a ratio of approximately 1:200 (drug:KBr) and compressed into pellets using the pellet press method. Individual pellets of 5-fluorouracil

(5-FU) and topotecan were prepared and analyzed over a wavelength range of 400–4000 cm^{-1} using an FTIR spectrophotometer.

X-ray Diffraction (XRD) Analysis:

X-ray diffraction analysis was carried out to assess the crystalline nature of the pure drug and excipients. The pure 5-FU exhibited distinct sharp diffraction peaks at 2θ values of 13.2° , 15.5° , 16.6° , 18° , and 23° , indicating its crystalline structure. Soya lecithin (30%) phospholipid displayed characteristic peaks at 2θ values of 11.3° and 23.5° . The crystalline pattern of the 5-FU mixture was clearly observed, confirming the retention of crystallinity, as shown in Figure 2.

In Vitro Drug Release:

The in vitro drug release profiles of 5-FU-loaded transfersomes, pure drug suspension, and the marketed formulation were evaluated in phosphate buffer solution (pH 5.5) at $37 \pm 0.5^\circ\text{C}$. The results of the release study are presented in Figure 3.

Release Kinetics of 5-FU-Loaded Transfersomes:

The release kinetics of the optimized 5-FU-loaded transfersomal formulation were analyzed using various mathematical models. The results indicated that the Higuchi model provided the best fit, with a correlation coefficient (R^2) of 0.987. This suggests that the drug release followed a diffusion-controlled mechanism, where the release is time-dependent and consistent with Fickian diffusion from a matrix-based system.

Drug Stability Studies:

The stability studies revealed a negligible increase in particle size, ranging from 35.45 ± 0.58 nm to 36.85 ± 3.43 nm, during storage at 4°C and 25°C . The initial entrapment efficiency (%EE) of the optimized transfersomal formulation remained relatively stable over the storage period.

Ex Vivo Skin Permeation Studies Using Confocal Laser Scanning Microscopy (CLSM):

The skin penetration ability of various transfersomal hydrogel formulations (PDH, MP, OTS, and TH) was evaluated using confocal laser scanning microscopy (CLSM). Goat skin was used as the model membrane due to its close resemblance to human skin in terms of physiological and structural properties. Each formulation was applied in vitro to goat skin to assess its permeation potential. Prior to CLSM analysis, the formulations were labeled with Rhodamine 123 to visualize and compare skin penetration efficiency.

RESULTS AND DISCUSSION

Optimization of Transfersomes and FTIR Spectral Analysis

The physical appearance of the optimized transfersome formulation is shown in Figure 1. The FTIR spectrum of pure 5-fluorouracil (5-FU) displayed characteristic peaks at 3736 cm^{-1} (N–H stretching), 1733 cm^{-1} (C=O stretching), and 1660 cm^{-1} (C=C stretching). A band attributed to C–H in-plane deformation appeared at 1568.6 cm^{-1} , and an out-of-plane deformation band was observed at approximately 399.19 cm^{-1} . Spectral data were collected with a resolution of 0.964 cm^{-1} .

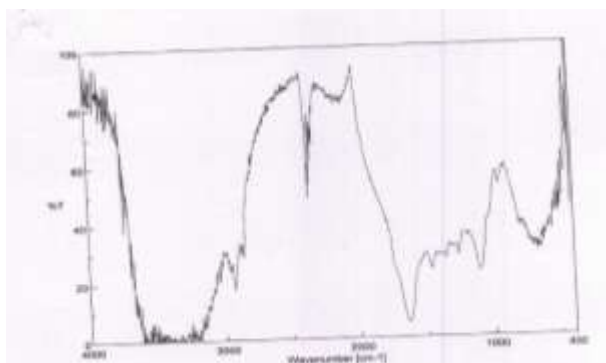


Figure 1: Optical approval for Transfersosomal preparation and FT-IR imigation

Entrapment Efficiency, Drug Loading, Zeta Potential, and Vesicle Size of Transfersomes:

The entrapment efficiency (%EE) of the deformable nanosized transfersomal vesicles ranged from $68.25 \pm 0.24\%$ to $85.05 \pm 0.58\%$, as shown in **Table 1**. A significant increase in %EE ($P < 0.05$) was observed with increasing concentrations of the edge activator (Tween 80) from 5% to 10% (w/w). However, further increasing the concentration to 15% (w/w) led to a significant reduction in %EE ($P < 0.05$). The optimal phospholipid-to-surfactant ratio of 90:10 (w/w) resulted in the highest entrapment efficiency (Table 1).

At lower concentrations, the incorporation of the edge activator resulted in an increase in vesicle size. However, at higher concentrations, the excess surfactant likely led to pore formation within the lipid bilayer,

compromising vesicle integrity. Additionally, concentrations above 15% may have promoted the formation of mixed micelles, which coexist with transfersomes and exhibit reduced drug entrapment due to their rigidity and smaller size [3, 9].

Patel et al. also reported that the ratio of soya lecithin (30%) to edge activator significantly influences the entrapment efficiency of lipophilic drugs like 5-fluorouracil. Excess surfactant disrupts lipid bilayer packing, thereby reducing encapsulation capacity. Drug loading was similarly affected by the composition of phospholipid and surfactant; in some formulations, an increase in both components resulted in improved drug loading, although the effect was limited and formulation-dependent. Overall, edge activator concentration had a statistically significant positive impact on drug loading efficiency.

The statistical model exhibited an F-value of 15.85, indicating strong significance. There is only a 0.08% probability that this F-value could occur due to random noise. A "Prob > F" value below 0.0500 confirms that the model terms are statistically significant.

Zeta potential values of the prepared formulations ranged from -9.22 mV to $+14.26$ mV, indicating good stability of the vesicular systems. The negative surface charge observed in most formulations suggests electrostatic repulsion, which contributes to colloidal stability. Vesicle size analysis, performed using a Malvern Mastersizer, revealed particle sizes ranging from 35.19 nm to 57.25 nm across different formulations.

Table 1: Different Adaptable factors also their determinestages with the help of Box-Behnken design model aimed at optimized of 5-FU entrapped transfersomes

| Adaptable factors | Stages | | |
|---|-----------|----------|----------|
| | -1 | 0 | 1 |
| Liberated Adaptable Factors | | | |
| X1= Soya Lecithin (30%) phospholipid: edge activator ratio, | 95:05:00 | 90:10:00 | 85:15:00 |
| X2= time will be need to sonication | 10min | 20min | 30min |
| X3= RPM (round per minute) | 20 | 40 | 60 |
| Deliberated Adaptable Factors | | | |
| Y1= particle size distribution (PSD) | minimize | | |
| Y2= %EE | maximize | | |
| Y3= %DL | constants | | |

Optimization Outcomes and Response Surface Analysis:

The results demonstrated minimal percentage bias, indicating consistency and reliability across the optimized formulations and confirming the suitability of the selected independent variables.

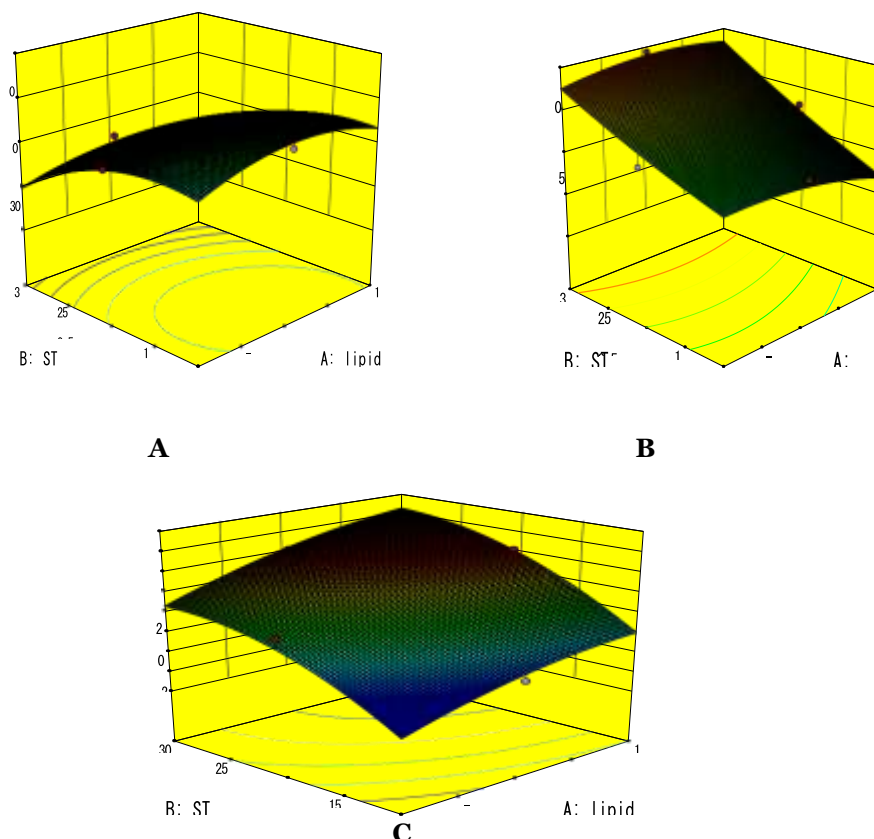


Figure 2 Fig. 9F-11. 3d Surface plots showing the effect of variables on (A) Particle Size (B) % Entrapment Efficiency and (C) % Drug loading.

The independent variables were defined as follows: **X₁** – ratio of soya lecithin (30%) to edge activator, **X₂** – sonication time, and **X₃** – rotational speed (RPM). These variables were assessed at three levels: –1 (low), 0 (medium), and +1 (high), representing the respective coded values.

The dependent responses included **Y₁** – particle size distribution (PSD), **Y₂** – entrapment efficiency (%EE), and **Y₃** – drug loading (%DL). These were optimized under specified constraints to enhance the performance of 5-FU-loaded transfersomal formulations.

Three-dimensional (3D) response surface plots were generated to evaluate the interaction effects of the independent variables on the measured responses. These graphical representations proved valuable in visualizing and understanding the relationships between formulation parameters and their influence on the outcome variables, thus aiding in the optimization process.

X-ray Diffraction (XRD) Study:

The XRD pattern of pure 5-fluorouracil (5-FU) exhibited sharp and well-defined peaks, indicating its crystalline nature, as shown in Figure 3. In contrast, the transfersomal formulation displayed broad, diffused peaks, reflecting a significant reduction in crystallinity. This decrease in diffraction intensity suggests that 5-FU was successfully encapsulated in an amorphous or less ordered form within the transfersomal vesicles.

In Vitro Drug Release:

In the in vitro drug release study, the cumulative percentage of drug release over 24 hours was evaluated for the optimized 5-FU-loaded transfersomal formulation, a pure drug suspension, and a marketed 5-FU product. The cumulative release values were found to be 61.68% for the transfersomal formulation, 70.85% for the pure drug suspension, and 74.85% for the marketed product, respectively. These results confirm the sustained release behavior of the transfersomal system compared to conventional formulations.

Drug Release Kinetics:

The release kinetics of the optimized transfersomal formulation were analyzed using various mathematical models. The best fit was observed with the Higuchi model, exhibiting a correlation coefficient (R^2) of 0.987, indicating that the drug release followed a diffusion-controlled mechanism. This model describes drug release from a matrix system where the release rate is time-dependent and governed by Fickian diffusion.

Stability Studies:

Stability studies of the optimized transfersomal formulation revealed only a minor increase in particle size, from 35.45 ± 0.58 nm to 36.85 ± 3.43 nm, during storage at 4°C and 25°C. The initial entrapment efficiency (%EE) was $84.54 \pm 0.52\%$. After six months of storage, the %EE decreased slightly to $81.52 \pm 0.65\%$ at 4°C and $78.88 \pm 0.46\%$ at 25°C. These results suggest that the formulation remained physically and chemically stable over the tested storage conditions.

Table 2: Actual experimental value design and expected values actual response.

| F. Code | X ₁ P/EA | X ₂ ST | X ₃ R | EE(%) | DL(%) | PDI | ZP(mV) |
|-------------|---------------------|-------------------|------------------|---------------------|----------------------|--------------------|--------------------|
| P-1 | 95:5(1) | 20 (0) | 60 (1) | 76.54 ± 0.21 | 8.015± 0.025 | 0.542±0.121 | 8.52±0.22 |
| P-2 | 95:5(1) | 30 (1) | 40 (0) | 73.52 ± 0.42 | 5.085± 0.006 | 0.452±0.452 | 7.51 ± 0.8 |
| P-3 | 85:15(-1) | 10 (-1) | 40 (0) | 69.08 ± 0.32 | 2.017± 0.124 | 0.331±0.521 | 5.23± 0.5 |
| P-4 | 85:15(-1) | 30 (1) | 40 (0) | 72.21 ± 0.84 | 0.351± 0.251 | 0.152±0.113 | 7.13 ± 0.2 |
| P-5 | 90:10(0) | 20 (0) | 40 (0) | 72.26 ± 0.52 | 3.275± 0.25 | 0.253±0.503 | 8.78 ± 0.3 |
| P-6 | 90:10(0) | 20 (0) | 40 (0) | 76.42 ± 0.14 | 2.017± 0.052 | 0.754±0.124 | 13.15± 0.2 |
| P-7 | 95:5(1) | 20 (0) | 20 (-1) | 79.56 ± 0.12 | 4.921± 0.057 | 0.157±0.542 | 11.52 ± 0.6 |
| P-8 | 85:15(0) | 20 (0) | 40 (0) | 69.95 ± 0.29 | 3.163± 0.231 | 0.325±0.542 | 9.65 ± 0.32 |
| P-9 | 95:5(1) | 10(-1) | 40 (0) | 68.25 ± 0.24 | 4.215± 0.026 | 0.252±0.142 | 13.25 ± 0.5 |
| P-10 | 85:15(-1) | 20 (0) | 20 (-1) | 72.52 ± 0.88 | 5.152± 0.055 | 0.523±0.521 | 8.52 ± 0.8 |
| P-11 | 90:10(0) | 20 (0) | 40 (0) | 71.86 ± 0.53 | 5.053± 0.028 | 0.523±0.521 | 10.52 ± 0.6 |
| P-12 | 90:10(0) | 30 (1) | 20 (-1) | 75.45 ± 0.85 | 2.052± 0.125 | 0.412±0.103 | 11.45 ± 0.5 |
| P-13 | 85:15(-1) | 20 (0) | 60 (1) | 75.69 ± 0.56 | 4.95 ± 0.052 | 0.54±0.542 | 7.52 ± 0.52 |
| P-14 | 90:10(0) | 20 (0) | 40 (0) | 72.52 ± 0.25 | 9.52 ± 0.415 | 0.595±0.254 | 10.15± 0.8 |
| P-15 | 90:10(0) | 10 (-1) | 20 (-1) | 77.58 ± 0.26 | 8.582 ± 0.089 | 0.458±0.854 | 11.85 ± 0.5 |
| P-16 | 90:10(0) | 30 (1) | 60 (1) | 85.05 ± 0.58 | 8.054 ± 0.152 | 0.285±0.125 | 14.50 ± 0.8 |
| P-17 | 90:10(0) | 10 (-1) | 60 (1) | 75.56± 0.57 | 0.026 ± 0.025 | 0.582±0.452 | 10.85 ± 0.54 |

P/EA= Phospholipid/Edge activator, ST= Sonication time, R= Revolution per minute

Comparative estimation of the experimental value and expected values in the planned below to experimental and expected conditions.

| Response Variable | Expected Values | Experimental Value | %Bias* |
|--------------------------|-----------------|--------------------|--------|
| ParticleSize(nm) | 32.96 | 35.58 | 7.94 |
| Entrapmentefficiency (%) | 86.06 | 85.45 | 0.70 |
| DrugLoading(%) | 8.81 | 8.054 | 8.58 |

*Bias was calculated as $[(\text{Expected Value} - \text{Experimental Value}) / \text{Expected value}] \times 100\%$.

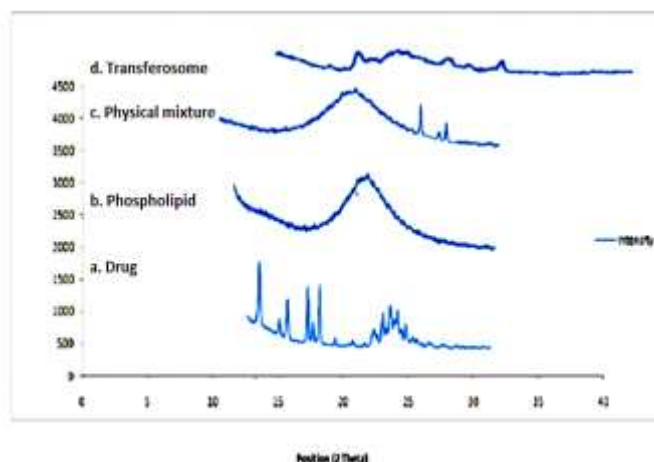


Figure 3 X-ray diffraction study of (a) 5-FU, (b) Soya Lacithin (30%) phospholipid, (c) Physical mixture and (d) Transfersome formulation

Ex-vivo Skin Permeation Studies

The skin penetration capability of various transfersosomal hydrogel formulations (PDH, MP, OTS, and TH) was evaluated using ex-vivo confocal laser scanning microscopy. Goat skin was chosen as the biological membrane for in-vitro studies due to its close resemblance to human skin in terms of physiological and structural characteristics.

To visualize skin penetration, all hydrogel formulations were pre-labeled with Rhodamine 123 (0.03% w/w) as a fluorescent marker. The prepared hydrogels were uniformly applied to the surface of the goat skin mounted on Franz diffusion cells. The receptor compartment was filled with phosphate buffer (pH 5.5), and the diffusion was allowed to occur for 24 hours.

After the exposure period, the skin samples were removed, gently washed with phosphate buffer to eliminate excess formulation, and immediately frozen using liquid nitrogen. Vertical skin sections (from stratum corneum to dermis) of approximately 250 μm thickness were obtained using a cryomicrotome (Leica, Germany). The tissue samples were embedded in a cryo-preserving medium and mounted on sample holders. Confocal laser scanning microscopy (Leica DMIRE2 with TCS SP2 system) was employed to scan the skin sections along the Z-axis in 15–30 nm increments, enabling visualization of the depth and extent of Rhodamine 123 penetration through the skin layers.

The drug release behavior observed in vitro suggested an initial burst release due to the availability of free 5-FU on the surface of the transfersomes. This was followed by sustained and prolonged release, attributed to the diffusion of 5-FU from the inner phospholipid bilayers of the vesicles. The formulation showed no signs of skin irritation and demonstrated effective retention and delivery of 5-FU across the skin barrier.

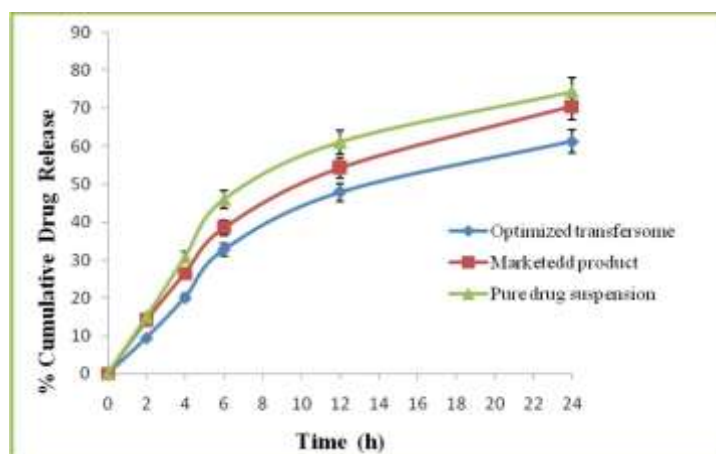


Figure 4. In vitro drug release profile of 5-FU entrapped transfersome & marketed formulation and pure drug suspension in skin pH 5.5.

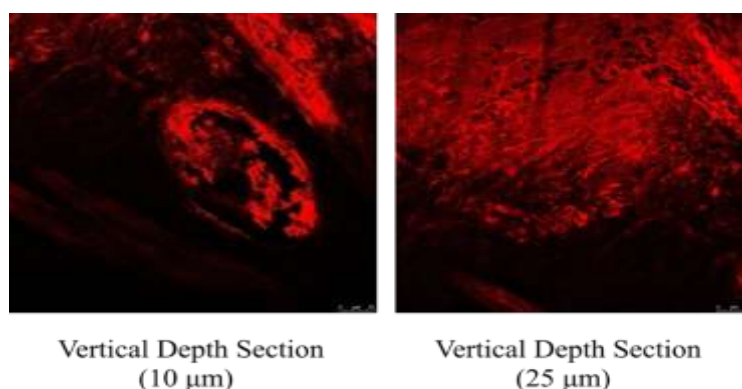


Figure 5: Showing Skin penetration ability of PDG formulations through Confocal solution Laser Microscopy at 0-10 μm and 0-25 μm

CONCLUSION

The 5-fluorouracil (5-FU) loaded transferosomal formulation using 30% soya lecithin demonstrated significant potential in the field of transdermal drug delivery. The optimized formulation (P-16) showed favorable physicochemical characteristics, with an average particle size of 35.58 ± 0.56 nm, a polydispersity index (PDI) of 0.285 ± 0.125 , and a zeta potential of $+14.50 \pm 0.8$ mV. The highest entrapment efficiency achieved was $85.05 \pm 0.58\%$ for the P-16 formulation.

When compared with a marketed formulation, the P-16 batch exhibited a 61% drug release, whereas the marketed product showed a release of 70%. Stability studies were conducted under various temperature and formulation conditions to assess physicochemical integrity. The optimization model yielded an F-value of 15.85, indicating high model significance, with only a 0.08% chance that this result was due to random variation. A "Prob > F" value below 0.0500 further confirmed the statistical reliability of the model.

FTIR analysis confirmed the structural integrity of 5-FU, showing characteristic peaks at 3736 cm^{-1} (N–H stretching), 1733 cm^{-1} (C=O stretching), and 1660 cm^{-1} (C=C stretching). X-ray diffraction (XRD) analysis of pure 5-FU displayed sharp peaks at 2θ values of 13.2° , 15.5° , 16.6° , 18° , and 23° , while soya lecithin exhibited characteristic peaks at 11.3° and 23.5° .

The drug release profile indicated an initial burst release phase within the first 2 hours, accounting for 10–15% release, attributed to surface-bound drug. This was followed by a sustained release from the vesicular core of the transfersomes. Overall, the transferosomal system offers a promising, cost-effective, non-toxic, and simple method for the transdermal delivery of 5-FU. Given these advantages, such formulations hold future potential for delivering various bioactive molecules.

ACKNOWLEDGMENT

The SAIF and my guide, Oriental University, Indore, as well as IISER Bhopal, supported X-ray diffraction analysis.

Source of support: Nil.

Conflict of interest: None

REFERENCES

1. Sağır T, Huysal M, Durmus Z, Kurt BZ, Senel M, Isik S. Preparation and in vitro evaluation of 5-fluorouracil loaded magnetite–zeolite nanocomposite (5-FU-MZNC) for cancer drug delivery applications. *Biomedicine & Pharmacotherapy*. 2016 Feb 1;77:182-90.
2. Cheng M, He B, Wan T, Zhu W, Han J, Zha B, Chen H, Yang F, Li Q, Wang W, Xu H. 5-Fluorouracil nanoparticles inhibit hepatocellular carcinoma via activation of the p53 pathway in the orthotopic transplant mouse model.
3. Singh S, Kotla NG, Tomar S, Maddiboyina B, Webster TJ, Sharma D, Sunnapu O. A nanomedicine-promising approach to provide an appropriate colon-targeted drug delivery system for 5-fluorouracil. *International Journal of Nanomedicine*. 2015 Nov 23;7:175-82.
4. Okada KI, Hirono S, Kawai M, Miyazawa M, Shimizu A, Kitahata Y, Ueno M, Hayami S, Yamaue H. Phase I Study of Nab–Paclitaxel plus Gemcitabine as Neoadjuvant Therapy for Borderline Resectable Pancreatic Cancer. *Anticancer Research*. 2017 Feb 1;37(2):853-8.
5. Han L, Tang C, Yin C. Dual-targeting and pH/redox-responsive multi-layered nanocomplexes for smart co-delivery of doxorubicin and siRNA. *Biomaterials*. 2015 Aug 1;60:42-52.
6. Xian XS, Park H, Choi MG, Park JM. Cannabinoid receptor agonist as an alternative drug in 5-fluorouracil-resistant gastric cancer cells. *Anticancer Research*. 2013 Jun 1;33(6):2541-7.
7. Patel R, Singh SK, Singh S, Sheth NR, Gendle R. Development and characterization of curcumin loaded

- transfersome for transdermal delivery. *Journal of pharmaceutical sciences and research*. 2009 Dec 1;1(4):71.
8. Nasr M, Ghorab MK, Abdelazem A. In vitro and in vivo evaluation of cubosomes containing 5-fluorouracil for liver targeting. *Acta pharmaceutica sinica B*. 2015 Jan 1;5(1):79-88.
 9. Duangjit S, Opanasopit P, Rojanarata T, Ngawhirunpat T. Characterization and in vitro skin permeation of meloxicam-loaded liposomes versus transfersomes. *Journal of drug delivery*. 2011;2011.
 10. Sabitha M, Rejinold NS, Nair A, Lakshmanan VK, Nair SV, Jayakumar R. Development and evaluation of 5-fluorouracil loaded chitin nanogels for treatment of skin cancer. *Carbohydrate polymers*. 2013 Jan 2;91(1):48-57.
 11. Palem CR, Dudhipala N, Battu SK, Goda S, Repka MA, Yamsani MR. Combined dosage form of pioglitazone and felodipine as mucoadhesive pellets via hot melt extrusion for improved buccal delivery with application of quality by design approach. *Journal of Drug Delivery Science and Technology*. 2015 Dec 1;30:209-19.
 12. Sarwa KK, Mazumder B, Rudrapal M, Verma VK. Potential of capsaicin-loaded transfersomes in arthritic rats. *Drug delivery*. 2015 Jul 4;22(5):638-46.
 13. Jangdey MS, Gupta A, Saraf S, Saraf S. Development and optimization of apigenin-loaded transfersomal system for skin cancer delivery: in vitro evaluation. *Artificial Cells, Nanomedicine, and Biotechnology*. 2017 Oct 3;45(7):1452-62.
 14. Jain SK, Gupta A. Development of Gelucire 43/01 beads of metformin hydrochloride for floating delivery. *AAPS PharmSciTech*. 2009 Dec;10:1128-36.
 15. Khan S, Boateng JS, Mitchell J, Trivedi V. Formulation, characterisation and stabilisation of buccal films for paediatric drug delivery of omeprazole. *Aaps Pharmscitech*. 2015 Aug;16(4):800-10.
 16. Alvi IA, Madan J, Kaushik D, Sardana S, Pandey RS, Ali A. Comparative study of transfersomes, liposomes, and niosomes for topical delivery of 5-fluorouracil to skin cancer cells: preparation, characterization, in-vitro release, and cytotoxicity analysis. *Anti-cancer drugs*. 2011 Sep 1;22(8):774-82.
 17. based quartz crystal microbalance biosensor for sensitive and selective detection of leukemia cells using silver-enhanced gold nanoparticle label. *Talanta*. 2014;126:130-5. <https://doi.org/10.1016/j.talanta.2014.03.056>
 18. Levitas VI, Samani K. Size and mechanics effects in surface- induced melting of nanoparticles. *Nature Communication*. 2011;2(1). <https://doi.org/10.1038/ncomms1275>.
 19. Aitken RJ, Chaudhry MQ, Boxall ABA, Hull M. Manufacture and use of nanomaterials: Current status in the UK and global trends. *Occupational Medicine*. 2006;56: 300-6. <https://doi.org/10.1093/occmed/kql051>.
 20. He H, Xie C, Ren J. Nonbleaching fluorescence of gold nanoparticles and its applications in cancer cell imaging. *Analytical Chemistry*. 2008;80(15):5951-7. <https://doi.org/10.1021/ac8005>